JME

Numerical modeling of hydraulic fracturing in carbonate rocks of Bangestan reservoir

A. Akrami, M. Hosseini* and H. Sodeifi

Department of Mining Engineering, College of Engineering, Imam Khomeini International University, Qazvin, Iran

Abstract

Hydraulic fracturing is used in the oil industry in order to increase the index of production and processing in the wells whose efficiencies have been dropped due to a long-term harvest or the rocks around the wells are of low permeability. Since the hydraulic fracturing operation is costly, it is of special importance to the project managers to determine the pressure required for hydraulic fracturing and the suitable pump for this operation. The numerical modelings used in this work are aimed to investigate the fracture pressure in the carbonate rocks of Bangestan reservoir in Ahvaz, Iran, and to determine a relationship between the pressure required for fracturing and the confining pressure. In this work, unlike the other ones in this field, the developed numerical models had no initial crack or fracture, and the path of the crack and how the crack grows were studied without any pre-determination and presumption. The results obtained show that, in most cases, the crack starts from the central part of the sample, and is extended to its two ends. The crack extension direction was along the borehole axis inside the sample and perpendicular to the lateral stress. The numerical modeling results were well-consistent with the experimental ones, indicating that the pump capacity constraints in the laboratory could be overcome through numerical modelings.

Keywords: *Hydraulic Fracturing, Numerical Modeling, Fracture Pressure, Extended Finite Element Method.*

1. Introduction

Hydraulic fracturing is used in the oil industry in order to increase the index of production and processing in the wells whose efficiencies have been dropped due to a long-term harvest or the rocks around the wells are of low permeability.

The hydraulic fracturing technique refers to the process of initiation and extension of fractures in rocks caused by the hydraulic pressure applied by a fluid. This technique was developed by Clark [1]. Haimson and Fairhurst continued the research on the initiation and extension of fracture [2]. Hubbert and Willis conducted comprehensive studies on the mechanics of hydraulic fracturing to determine the direction and condition of the principal stresses using the hydraulic fracturing process [3]. Since then, numerous studies and modellings have been conducted to investigate the factors affecting the hydraulic fracturing. A number of these studies were discussed as what follow.

Riberio et al. have designed a three-axis load cell system quipped with a system to apply a borehole pressure and a pressure recording system for experimental modeling of hydraulic fracturing. The cell had a capacity of 21 MPa for the axial loading and 10.5 MPa for lateral loading. The studied samples were cubic and made of gypsum in small-scale ($0.1 \times 0.1 \times 0.1$ m^3). The results obtained indicate the efficiency of this cell in hydraulic fracturing modeling [4].

Song et al. have conducted experimental studies on sandstone samples. They aimed to investigate the fracture pressure in the hydraulic fracturing test, and present a proper relationship between the fracture pressure and the confining pressure in high-permeability sandstones [5].

De pater and Beugelsdijk have experimentally and numerically modeled the hydraulic fracturing process in naturally-fractured rocks. They found that at low flow rates, injection always led to fluid flow in natural fractures. New fractures could propagate at higher flow rates. High flow rates or high viscosity caused a failure, while low flow rates opened the failure network [6].

Satoh and Yamaguchi It should be noted that in the first four models, experimental modeling along with numerical modeling was conducted to validate the results.

experimentally modeled hydraulic fracturing in the materials used inside the core of embankment dams. The experiments were conducted on hollow cylindrical samples (large-scale samples with outer diameter of 30 cm and medium-scale samples with outer diameter of 15 cm). The effect of maximum soil grain diameter, D_{max}, and confining pressure, σ_3, on the fracture pressure and strength of samples made from compacted materials against hydraulic fracturing was studied. They also presented a graph that demonstrated the relationship between the fracture pressure, P_f, and the confining pressure, $\sigma3$, for hydraulic fracturing experiments in embankment dam core materials with different particle diameters [7].

Carvalho et al. have conducted a numerical modeling using the finite element method for vertical wells in order to examine the extension of vertical hydraulic fractures. They also performed a parameter study to analyze the effect of layering of formation and characteristics of different materials layered around the fractures on the pressure of hydraulic fracturing [8].

Shimizu et al. have investigated the hydraulic fracturing in hard rocks, considering the fluid viscosity and particle size distribution. Their results showed that for all samples, the direction of hydraulic fractures was parallel to the maximum principal stress. The fracture pressure for a low-viscosity fluid was lower than that for a high-viscosity fluid. A low-viscosity fluid was found to be able to easily penetrate the fracture [9].

Chen has introduced the application of the extended finite element method for the hydraulic fracturing problems, and compared and evaluated the modeling results using this method using the finite element method and analytic equations. The preliminary results obtained in that study were one of the first steps in the application of the extended finite element method in modeling hydraulic fracturing [10].

Zhao et al. have conducted a numerical modeling for hydraulic fracturing using a combination of discrete element method and the finite element method. The modeling showed that at small-scale, hydraulic fractures tend to propagate in the rock discontinuities, while in the reservoir scale, hydraulic fractures propagate in the direction of the maximum principal stress [11].

In general conditions, the fracture pressure is not dependent only upon confining pressure. Basically, it is dependent on confining pressure (in the condition when minimum horizontal stress is equal to maximum horizontal stress), pore pressure, and tensile strength; previous studies have confirmed this [7, 12-15]. However, here, in this research work, the pore pressure is zero and the tensile strength is constant because the tests have been conducted on samples of one type of rock. Therefore, in this work, the fracture pressure was only dependent on confining pressure.

The simulations were carried out on a thick-walled hollow cylinder.

A hollow cylinder with inner radius R_i, outer radius R_o, uniform internal pressure P_i, confining pressure P_o, and axial force P is shown in Figure 1. In cylindrical coordinates (r, θ, z), stresses σ_r and σ_θ anywhere with radial distance (r) from the center of the sample were calculated using Equations (1) and (2) [16]:

$$\sigma_r = \frac{P_O R_O^2 - P_i R_i^2}{R_O^2 - R_i^2} - \frac{(P_O - P_i) R_i^2 R_O^2}{r^2 (R_O^2 - R_i^2)} \quad (1)$$

$$\sigma_\theta = \frac{P_O R_O^2 - P_i R_i^2}{R_O^2 - R_i^2} + \frac{(P_O - P_i) R_i^2 R_O^2}{r^2 (R_O^2 - R_i^2)} \quad (2)$$

In this case, the axial stress σ_z was obtained from Equation (3):

$$\sigma_Z = \frac{F}{\pi (R_O^2 - R_i^2)} - \frac{P_i R_i^2}{R_O^2 - R_i^2} \quad (3)$$

Compared to the previous studies, the innovation of this work could be described from the experimental and numerical aspects. From the former perspective, this study made modifications to the Hoek triaxial cell, which is available in most rock mechanics laboratories. This modified cell can be used to carry out hydraulic fracturing tests when the horizontal stresses in a well are isotropic, i.e. are equal (horizontal stresses are mostly equal in deep production wells). From a numerical perspective, the extended finite element method (XFEM) was used in this work. Ultimately, a relation was presented to estimate

the fracture pressure based on the applied confining pressure by numerical modeling. These models can be used to select the appropriate pump to conduct the hydraulic fracture operations in situ conditions.
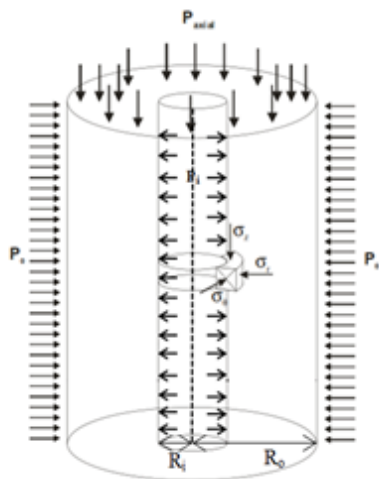

Figure 1. A view of a thick-walled cylinder under internal pressure, lateral stress, and axial stress [17].

2. Samples
The studied carbonate samples were collected from one of the wells in an Ahvaz oil field located in SW Iran, which was drilled for oil production in the southern slopes of the Bangestan reservoir. The characteristics of the rock samples are listed in Table 1. The ISRM standard was used for determining these properties [18-21].

3. Extended finite element method
A majority of the previous studies used the finite element method (FEM), boundary element method (BEM), and finite difference method (FDM) in this regard. Having many advantages over the previous methods, XFEM is one of the newest methods used in modeling fracture mechanics. Modeling discontinuities such as cracks using the conventional FEM and BEM requires the grid to adapt to the geometry of the discontinuity. Therefore, these two methods use considerably fine meshes or singular elements in the crack tip. Modeling a growing crack involves even further complexities since the grid should be capable of adapting itself with the new geometry of the crack as it grows. XFEM, which is based upon the conventional FEM, employs specific functions known as enrichment functions in the standard numerical solution depending on the type of discontinuities. In XFEM, the crack growth is modeled by adding degrees of freedom to the nodes around a crack [23].
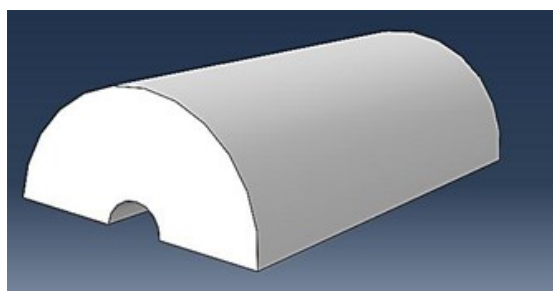
Table 1. Physical and mechanical characteristics of studied rock samples.

Density (KN/m^3)	Effective porosity (%)	Uniaxial compressive strength (MPa)	Tensile strength (MPa)	Elastic modulus (GPa)	Poisson ratio	Fracture energy* (N/m)
20.91	0.81	94.27	4.3	32.43	0.294	20

(*Definition of fracture energy: $G_{IC} = K_{IC}^2 / E$ where: K_{IC} and E are mode I fracture toughness and modulus of elasticity, respectively [22].)

3.1. Model geometry
ABAQUS 6.12 was used for modeling. This version of the software is based upon the finite element method.
The model was a thick-walled hollow cylinder with an outer diameter of 54.7 mm and a height of 108 mm with a central hole with a diameter of 12 mm. Since the model was symmetrical, the model geometry was regarded as a half-cylinder to reduce the analysis time (Figure 2). The model had no initial crack or fracture, and no pre-determinations were made regarding the path and characteristics of the crack.

Figure 2. Geometry of developed model.

3.2. Damage criterion

The maximum principal stress criterion, implemented in ABAQUS, was used to predict the fracture path in the 3D models developed in this work. The criterion is defined based on Equation (4):

$$f = \left\{ \frac{\sigma_{max}}{\sigma_{max}^o} \right\} \tag{4}$$

where σ_{max}^0 denotes the maximum allowed principal stress. The symbol $\Leftrightarrow$ is known as the Macaulay parentheses. When the argument of the function is negative, the function returns to zero, and when the argument is positive, the function equals its argument. Therefore, compressive stress cannot cause damage. Damage begins when f in Equation (4) reaches 1. The developed crack or the initial crack is extended when after a stage of balance, the failure criterion lies in the ranged specified in Equation (5) according to the considered tolerance (f_{tol}) (ABAQUS 6.10 documentation, ABAQUS theory manual) [24]:

$$1.0 \le f \le 1.0 + f_{tol} \tag{5}$$

3.3. Loading and boundary conditions

In this model, three loadings including axial and lateral loadings and borehole fluid loading were applied to the sample. The axial and lateral loadings increased statically, while borehole loading increased linearly. Boundary conditions were determined based on the position of the sample faces. Figure 3 shows the axial and lateral loadings as well as the boundary conditions, and Figure 4 shows the borehole fluid loading. A linearly-increased pressure was applied to the borehole fluid. The test procedure was added to the paper. In each test, at first, the axial stress and the confining pressure were increased to a specified value, and then during the test, the axial stress and the confining pressure were maintained at the same value. In the next step, the borehole pressure was increased. The stress rate for borehole pressure was 0.5 MPa/s.

3.4. Meshing of model

Tetrahedral elements and the free meshing technique were used in this work. Figure 5 shows the meshing of the model.
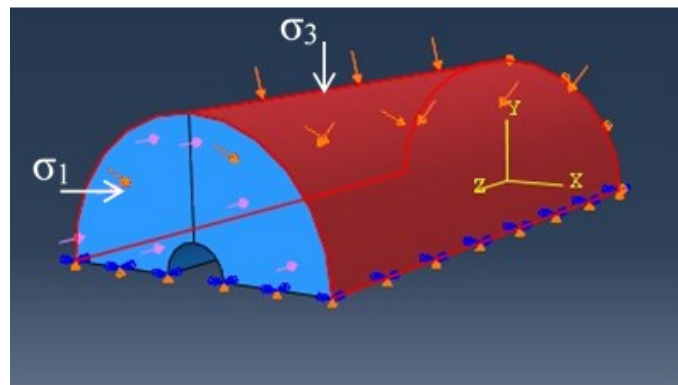

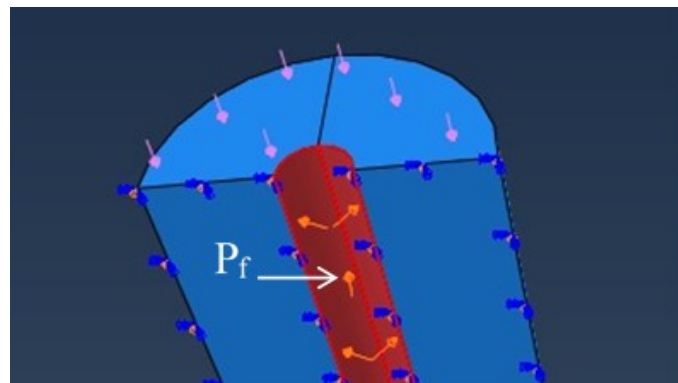**Figure 3. Axial and lateral loadings and boundary conditions.**

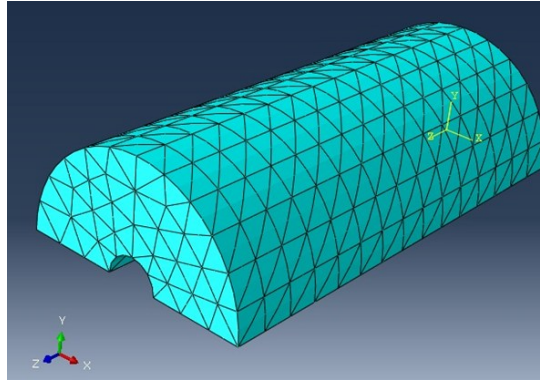**Figure 4. Loading of borehole fluid.**

Figure 5. Meshing of model.

3.5. Modeling results

A total of 10 models with different lateral and axial stresses were developed in this work. In these models, the ratio of axial stress to lateral stress was considered to be 3.5. Figure 6 shows the principal stresses at the fracture initiation for sample 5. Figure (6-A) represents the maximum principal stress at initiation of the fracture. The maximum principal stress at the fracture initiation point was determined to be 9 MPa and tensile, and the maximum principal stress at the outer wall of the sample was 8.55 MPa and compressive (the negative and positive signs correspond to compression and tension, respectively). Figure (6-B) shows the average principal stress at the fracture initiation. The average principal stress at the fracture initiation point was 25 MPa and compressive, and the maximum principal stress at the outer wall of the sample was 9.9 MPa and tensile. Figure (6-C) shows the minimum principal stress at the fracture initiation. The stress was determined to be 35 MPa and compressive.

Figure 7 shows the total displacements at the fracture initiation point for samples 5 and 9. In sample 5, the total displacement at the crack was 0.53 mm. In sample 9, the total displacement was 9.2 mm.

Figure 8 illustrates the crack extension direction in sample 5.
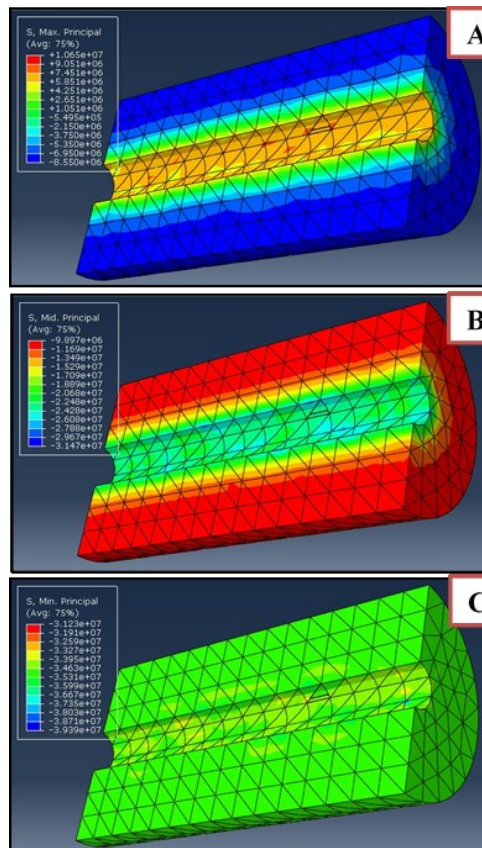

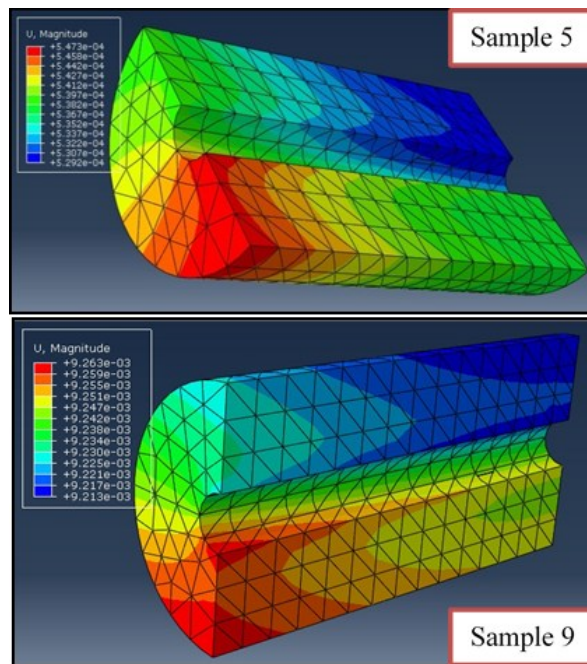**Figure 6. Principal stresses in sample 5.**

Figure 7. Total displacements at fracture initiation point for samples 5 and 9.
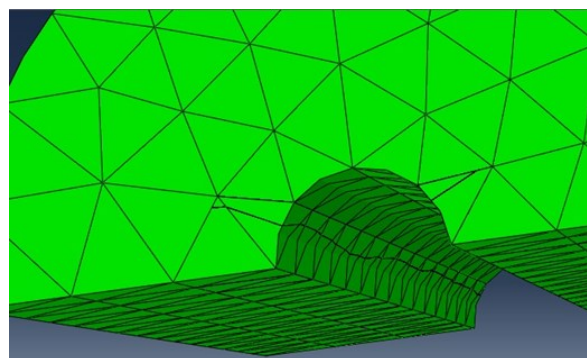

Figure 8.Crack extension direction in sample 5.

The fracture pressures in the developed models are listed in Table 2. The Fracture pressures obtained from numerical modeling had a 10% difference with the experimental modeling results (Figure 9). This difference could be due to the presence of micro-cracks in the real samples, while in numerical modeling, samples are considered homogeneous, uniform, and without micro-cracks. It should be noted that in the first four models, experimental modeling along with numerical modeling was conducted to validate the results.

Table 2. Numerical modeling results.

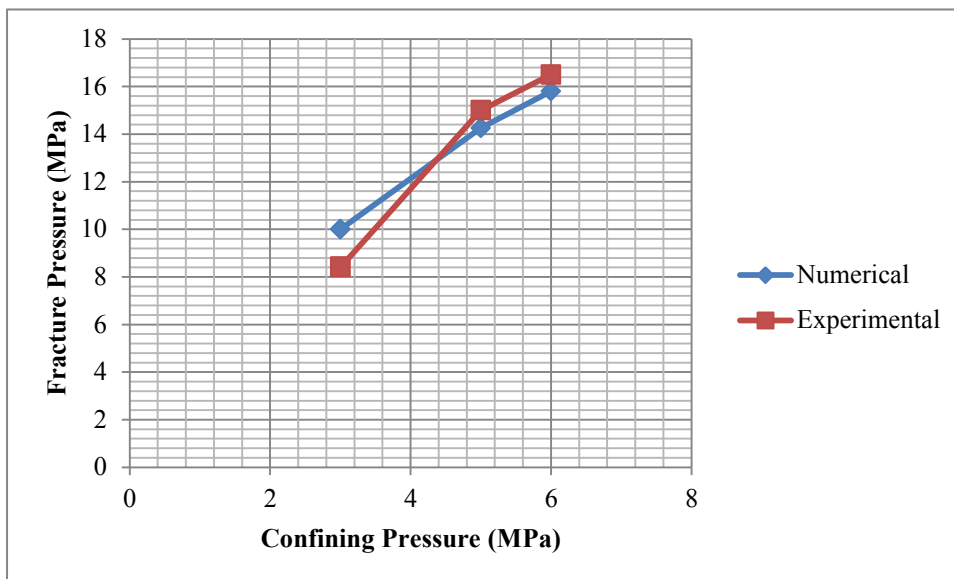| Model number	Axial stress (MPa)	Confining pressure (MPa)	Fracture pressures obtained from numerical modeling	Fracture pressures obtained from experimental modeling
1	10.5	3	10	8.43
2	17	5	14.25	15
3	19.2	6	15.8	16.49
4	13.5	3	10	8.41
5	35	10	25.5	-
6	70	20	46	-
7	105	30	67	-
8	140	40	86	-
9	175	50	107	-
10	210	60	127.5	-

Figure 9. Comparison of pressure magnitudes required for fracture in experimental modeling and numerical modeling.

Figure 10 shows the relationship between the pressure required to initiate hydraulic fracturing and confining pressure for carbonate rocks is the Bangestan reservoir. There was an almost linear relationship between the fracture pressure and the confining pressure. Thus with an increase in the confining pressure, the pressure required to initiate hydraulic fracturing increased. The relationship between the fracture pressure and the confining pressure for carbonate rocks in the

Bangestan formation is in the form of Equation (6).

$$P_f = 2.0605\,\sigma_3 + 4.1326 \qquad (6)$$

In this research work, the effects of elastic modulus and Poisson's ratio on the fracture pressure were investigated using numerical modelings. The results of these numerical modelings are listed in Table 3.
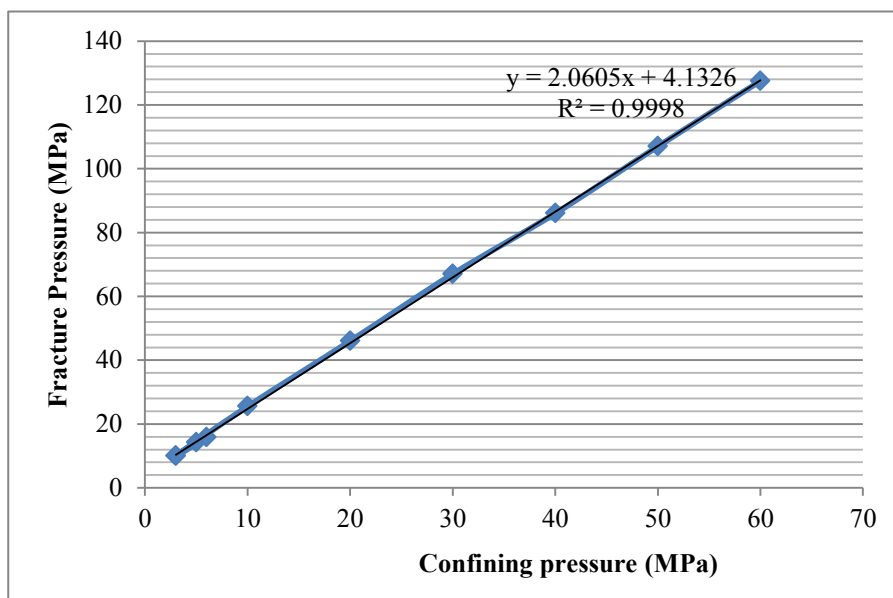

Figure 10. Graph of pressure required for fracture initiation by confining pressure.

Table 3. Numerical modeling results.

Model number	Elastic modulus (GPa)	Poisson's ratio	Fracture pressure (MPa)
1	32.43	0.294	10
2	42.15	0.294	10.09
3	22.7	0.294	9.96
4	32.43	0.2	10.40
5	32.43	0.147	10.80

Model number 1 is related to the numerical modeling with characteristics of the rock samples of the Bangestan reservoir. The numerical modeling (in models numbers 2 and 3) was carried out to investigate the effect of elastic modulus on the fracture pressure. As it could be seen, with the change in the elastic modulus up to 50%, the fracture pressure was not significantly affected. These results are consistent with the results obtained by Shafaei-Zadeh et al. [23]. The numerical modeling (in models numbers 4 and 5) was carried out to investigate the effect of Poisson's ratio on the fracture. The results obtained from numerical modeling also showed that the fracture pressure decreased with increase in the Poisson's ratio. The fracture pressure increased to 8% by decrease in the Poisson's ratio up to 50%. These results are consistent with the results obtained by Moazami Godarzi et al. [25]. The axial stress and the confining pressure in all

of the numerical modelings were 3 and 1.5 MPa, respectively.

4. Analysis of results

Satoh and Yamaguchi have conducted a research work on the relationship between the fracture pressure and the confining pressure [7]. They experimentally modelled hydraulic fracturing for the materials used in the core of embankment dams. They presented a graph that demonstrated the relationship between the fracture pressure, P_f, and the confining pressure, σ_3, for hydraulic fracturing tests in the materials used in the core of embankment dams with different particle diameters. Figure 11 shows the graph presented by Satoh and Yamaguchi. As it can be seen, the relationship presented by them is linear, similar to the relationship obtained here.
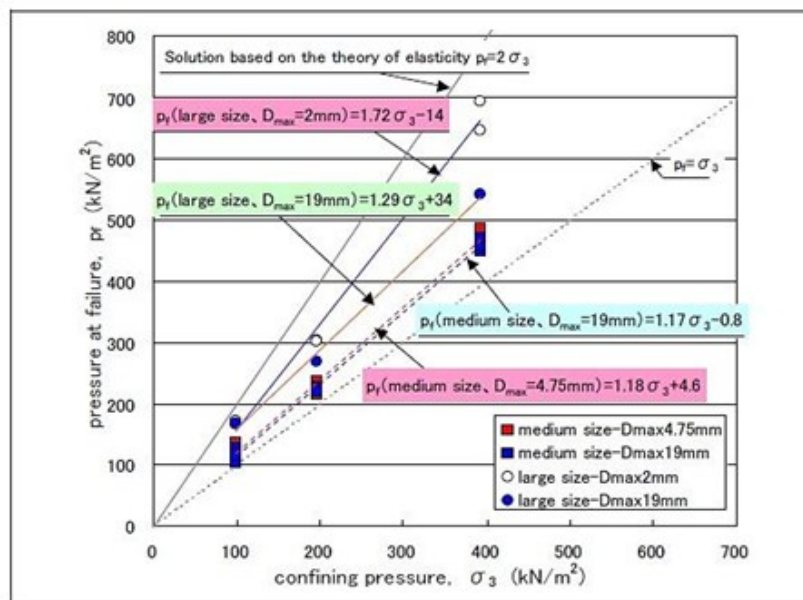

Figure 11. Relationship between fracture pressure and confining pressure [7].

The laboratory studies carried out by Song et al. (2001) and Chet et al. (2004) also showed that the relationship between the fracture pressure and the confining pressure was linear [5, 15]. In these tests, the effective confining pressure reached 35 MPa.

The experimental and numerical modelings show that, in terms of geometry, hydraulic fracturing is such that fractures are often directed vertically (along the axis of the sample). Given that in this modeling the applied axial stress was greater than the lateral stress, it could be concluded that the

direction of fractures must always be parallel to the maximum principal stress and perpendicular to the horizontal stress. This is consistent with the theories presented by Hubert Willis. According to the Griffith's criterion, in uniform and isotropic rocks, if the borehole axis is parallel to one of the principal stresses, fractures resulting from hydraulic fracturing extend parallel to the maximum principal stress and perpendicular to the horizontal stress.

Comparing the total displacement in the two samples 5 and 9, it was found that with an increase in the lateral stress, the displacements at the moment of fracture would increase.

The values obtained for fracture pressure in the experimental and numerical modelings show that with an increase in the lateral stress, the fracture pressure will also increase. However, in experiments 1 and 4, where the lateral stress was constant, despite the significant differences in the axial stress in the two experiments (3 MPa), their corresponding fracture pressures were slightly different. Therefore, it can be concluded that the fracture pressure caused by hydraulic fracturing is mostly affected by the lateral stress and less affected by the axial stress. The increased fracture pressures caused by an increase in the lateral stress can be explained using the stress distribution in a hollow cylinder.

According to Equation (2), an increase in the lateral tension (P_O) will lead to the increase in the tangential stress (σ_θ), which is compressive. Thus a higher fluid borehole pressure is required for the tangential stress in the inner cylinder wall to become tensile and fracture the wall. As it can be seen, the axial stress (σ_z) does not affect the tangential stress and, thereby, the fracture pressure.

In the numerical modeling, the extended finite element method based on the maximum principal stress (MAXPS as a damage criterion for the traction separation) criterion was used to initiate and grow cracks. According to the stress distribution in the hollow cylinder, the inner wall of the cylindrical sample was under a tensile stress. Therefore, the maximum principal stress value was considered equal to the tensile strength of carbonate rocks.

5. Conclusions

The hydraulic fracture process has been extensively used in different engineering areas in the past decades. In the petroleum industries, this technique is employed to form significantly large cracks with a high hydraulic conductivity in order to increase the rates of oil and gas flows from hydrocarbon reservoirs with a low penetrability towards drilled wells. The present work experimentally and numerically modeled the hydraulic fracture operation for carbonate rocks of the Bangestan reservoir in Ahvaz, Iran. The experimental modelling was carried out using the triaxial Hoek cell. A number of parts were designed, built, and added to the cell in order to prepare it for modeling the hydraulic fracture process. The fracture pressure can be measured in this model. Moreover, the numerical modeling was conducted using the ABAQUS software package so that the high lateral fracture pressures could be calculated through this model when the laboratory pump failed to break the sample rock.

The results of the present work on carbonate rocks showed that:

1. The results of numerical modeling were consistent with those of the experimental modeling. In all the experiments and modelings, the developed fractures were vertical (along the axis of the sample) or nearly vertical. This is consistent with the theories presented in this field.

2. The increase in the lateral stress led to an increase in the fracture pressure (according to Equation 6). However, changes in the axial stress did not significantly change the fracture pressure. This observation can also be explained based on the stress distribution in the hollow cylindrical samples.

3. The fracture pressure has an inverse relationship with the Poisson's ratio.

4. The fracture pressure has nothing to do with the elastic modulus.

5. Unlike other studies conducted in this field, the numerical modeling in this work was performed without any initial pre-determinations for the crack-less models. The results obtained show that, in most cases, the cracks initiate from the center and are extended toward both ends of the sample. The crack extension direction was parallel to the borehole axis inside the sample and perpendicular to the lateral stress. This is fully consistent with the observation in the experimental models.

6. Finally, an empirical relationship between the fracture pressure and the confining pressure for carbonate rocks in the Bangestan formation was presented using a numerical modeling. Furthermore, these results were validated through an experimental modeling. This relationship was linear and could be used to select a suitable pump for hydraulic fracturing in this reservoir.

References

[1]. Clarck, J.B. (1949). A Hydraulic process for increasing the productivity of wells. Petroleum Division Fall Meeting. Dallas. Texas.

[2]. Haimson, B.C. and Fairhurst, C. (1967). Initiation and extension of hydraulic fracturing in rocks. Soc. Petrol. Engrs. J. Sept. pp. 310- 318.

[3]. Hubbert, M.K. and Willis, D.G. (1957). Mechanics of hydraulic fracturing. Trans. AIME 210. pp. 153-166.

[4]. Ribeiro, P.R., de Oliveira e Sousa, J.L.A., Fernandes, P.D. and Caldas Leite, V.L. (1999). Hydraulic fracturing physical simulation. 15th Brazilian congress of mechanical engineering. Sao Paulo.

[5]. Song, I., Suh, M., Won, K.S. and Haimson, B. (2001). A laboratory study of hydraulic fracturing breakdown pressure in tablerock sandstone. Geosciences Journal. 5 (3): 263-271.

[6]. De pater, C.J. and Beugelsdijk, L.J.L. (2005). Experiments and numerical simulation of hydraulic fracturing in naturally fractured rock. presented at Alaska Rocks. The 40th U.S. Symposium on Rock Mechanics.

[7]. Satoh, H.S. and Yamaguchi, Y. (2008). Laboratory Hydraulic Fracturing Tests For Core Materials Using Large Size Hollow Sylinderical Specimens. The 1st International Symposium on Rockfill Dams.

[8]. Carvalho, E.C., Bendezu, M.A.L., Oliveira, M., Roehl, D.M. and Sousa, L. (2010). Finite Element Modeling of Hydraulic Fracturing in Vertical Wells. Mecânica Computacional. 29: 8571-8578.

[9]. Shimizu, H., Murata, S. and Ishida, T. (2011). The distinct element analysis for hydraulic fracturing in hard rock considering fluid viscosity and particle size distribution. International Journal of Rock Mechanics and Mining Sciences, 48 (5): 712-727.

[10]. Chen, Z. (2013). Implementation of the XFEM for Hydraulic Fracture Problems. 13th International Conference on Fracture. Beijing. China.

[11]. Zhao, Q., Lisjak, A., Mahabadi, O., Liu, Q. and Grasselli, G. (2014). Numerical simulation of hydraulic fracturing and associated microseismicity using finite-discrete element method. Journal of Rock Mechanics and Geotechnical Engineering. 6: 574-581.

[12]. Ghanbari, A. and Rad, S.S. (2015). Development of an empirical criterion for predicting the hydraulic fracturing in the core of earth dams. Acta Geotechnica. 10 (2): 243-254.

[13]. Jaworski, G.W., Duncan, J.M. and Seed, H.B. (1981). Laboratory study of hydraulic fracturing. J Geotech Eng Div ASCE. 107 (6): 713-732.

[14]. Mori, A. and Tamura, M. (1987). Hydrofracturing pressure of cohesive soils. Soil Found Jpn Soc Soil Mech Found Eng. 27 (1): 14-22.

[15]. Chen, M. and Zhang, G.Q. (2004). Laboratory measurement and interpretation of the fracture toughness of formation rocks at great depth. Journal of Petroleum Science and Engineering. 41: 221-231.

[16]. Hoek, E. and Franklin, J.A. (1967). A simple triaxial cell for field or laboratory testing of rock. Imperial College of Science and Technology. University of London.

[17]. Elkadi, A. and Van Mier, J. (2004). Scaled hollow-cylinder tests for studying size effect in fracture processes of concrete. Fracture mechanics of concrete structures.1: 229-236.

[18]. Franklin, J. A. (1979). Suggested methods for determining water-content, porosity, density, absorption and related properties and swelling and slake-durability index properties. 1. Suggested methods for determining water-content, porosity, density, absorption and related properties. International Journal of Rock Mechanics and Mining Sciences, 16 (2): 143-151.

[19]. Bieniawski, Z.T. and Bernede, M.J. (1979, April). Suggested methods for determining the uniaxial compressive strength and deformability of rock materials: Part 1. Suggested method for determining deformability of rock materials in uniaxial compression. In International Journal of Rock Mechanics and Mining Sciences & Geomechanics Abstracts 16 (2): 138-140.

[20]. ISRM. (1978). Suggested methods for determining tensile strength of rock materials. Int J Rock Mech Min Sci Geomech Abstr. 15: 99-103.

[21]. Kuruppu, M.D., Obara, Y., Ayatollahi, M.R., Chong, K.P. and Funatsu, T. (2014). ISRM-Suggested Method for Determining the Mode I Static Fracture Toughness Using Semi-Circular Bend Specimen. Rock Mechanics and Rock Engineering. 47: 267-274.

[22]. Bazant, Z.P. and Kazemi, M.T. (1990). Determination of fracture energy, process zone length and brittleness number from size effect. With application to rock and concrete International Journal of Fracture. 44: 111-131.

[23]. Shafaei-Zadeh, A., Forouzan, M.R. and Faramarzi, L. (2014). Simulation of crack initiation and extension in hydraulic fracturing of oil wellbore using maximum principal stress criterion. Modarres Mechanical Engineering Journal. 14 (5): 164-176.

[24]. Abaqus 6.10 documentation. Abaqus theory manual.

[25]. Moazami Godarzi, H., Ahangari, K. and Sheikh Zakariayi, S.J. (2014). The effect of Poisson's ratio on the fracture pressure in operation hydraulic fracturing. Second National Iranian Oil and Gas Conference.

مدل‌سازی عددی شکست هیدرولیکی در سنگ‌های کربناته ی مخزن بنگستان

عباس اکرمی، مهدی حسینی* و هوتن سدیفی

گروه مهندسی معدن، دانشکده فنی و مهندسی، دانشگاه بین‌المللی امام خمینی (ره)، ایران

* نویسنده مسئول مکاتبات: ma.hosseini@eng.ikiu.ac.ir

چکیده:

در صنعت نفت به منظور افزایش شاخص تولید و بازیافت از چاه‌هایی که به علت برداشت طولانی مدت، بازده آن کاهش یافته است یا سنگ‌های اطراف چاه، میـزان نفوذپذیری کمی دارند از شکست هیدرولیکی استفاده می‌شود. از آنجایی که عملیات شکست هیدرولیکی، عملیاتی پر هزینه است، به دست آوردن فشار لازم بـرای شکست هیدرولیکی و تعیین پمپ مناسب برای این عملیات، برای مجریان پروژه اهمیت به سزایی دارد. هدف از این مدل‌سازی‌ها، بررسـی فشـار شکسـت در ایـن مخزن و به دست آوردن رابطه‌ای بین فشار لازم برای شکست و فشار محصور کننده است. در این پژوهش بر خـلاف دیگـر تحقیقـات انجـام شـده در ایـن زمینـه، مدل‌های عددی ساخته شده بدون ترک و شکستگی پیش فرض بوده و مسیر و نحوه‌ی رشد ترک بدون هیچ پیش داوری و تعیین قبلی مورد بررسی قـرار گرفـت. نتایج نشان داد که در اغلب موارد، ترک از قسمت مرکزی نمونه آغاز شده و به سمت دو سر نمونه گسترش می‌یابـد و راسـتای گسـترش تـرک در راسـتای محـور گمانه‌ی داخل نمونه و عمود بر تنش جانبی است. نتایج به دست آمده از مدل‌سازی‌های عددی مطابقت خوبی با نتایج مدل‌سازی‌های آزمایشگاهی دارد و مـی‌تـوان محدودیت ظرفیت پمپ موجود در آزمایشگاه را با مدل‌سازی عددی جبران کرد.

کلمات کلیدی: شکست هیدرولیکی، مدل‌سازی عددی، فشار شکست، روش المان محدود توسعه‌یافته.